

Data supplement to “Phase resolved simulation of the Landau-Alber stability bifurcation”

Agissilaos G. Athanassoulis¹

¹Department of Mathematics, University of Dundee

Friday 30th December, 2022

Consider a background solution of the NLS

$$iu_t + p\Delta u + q|u|^2u = 0, \quad u(x, 0) = u_0(x) \quad (1)$$

where $u_0(x)$ is a typical realisation of a sea state with known power spectrum. Then one can consider adding a small, localised perturbation, $u_0(x) \mapsto u_0(x) + \delta_0(x)$. This would give rise to the initial value problem of finding $v(x, t)$ such that

$$iv_t + p\Delta v + q|v|^2v = 0, \quad v(x, 0) = u_0(x) + \delta_0(x). \quad (2)$$

By taking the difference, we can recover the inhomogeneity $\delta(x, t)$,

$$\delta(x, t) := v(x, t) - u(x, t). \quad (3)$$

Seven scenarios are ran, each for a JONSWAP sea state, parametrised by $j = 1, \dots, 7$. The following figures illustrate the onset of modulation instability. Observe how the values of the inhomogeneity are smaller than the background solution for the stable cases $j = 1$ through 3, and larger for $j = 5$ through 7. Also note how the extreme events that are produced in the unstable cases are localised, although not exclusively in the area of the original inhomogeneity (especially for the more unstable cases). See figures 1 through 7.

Note that the data saved in this repository are on a time grid coarser than the one used in computation for space reasons. The time and space grid is also included, as are the initial conditions. The notations are identical as in the paper. The format is MATLAB .mat files.

Please consult [1] for more details.

References

- [1] A.G. Athanassoulis, “Phase resolved simulation of the Landau-Alber stability bifurcation”, Fluids, accepted for publication

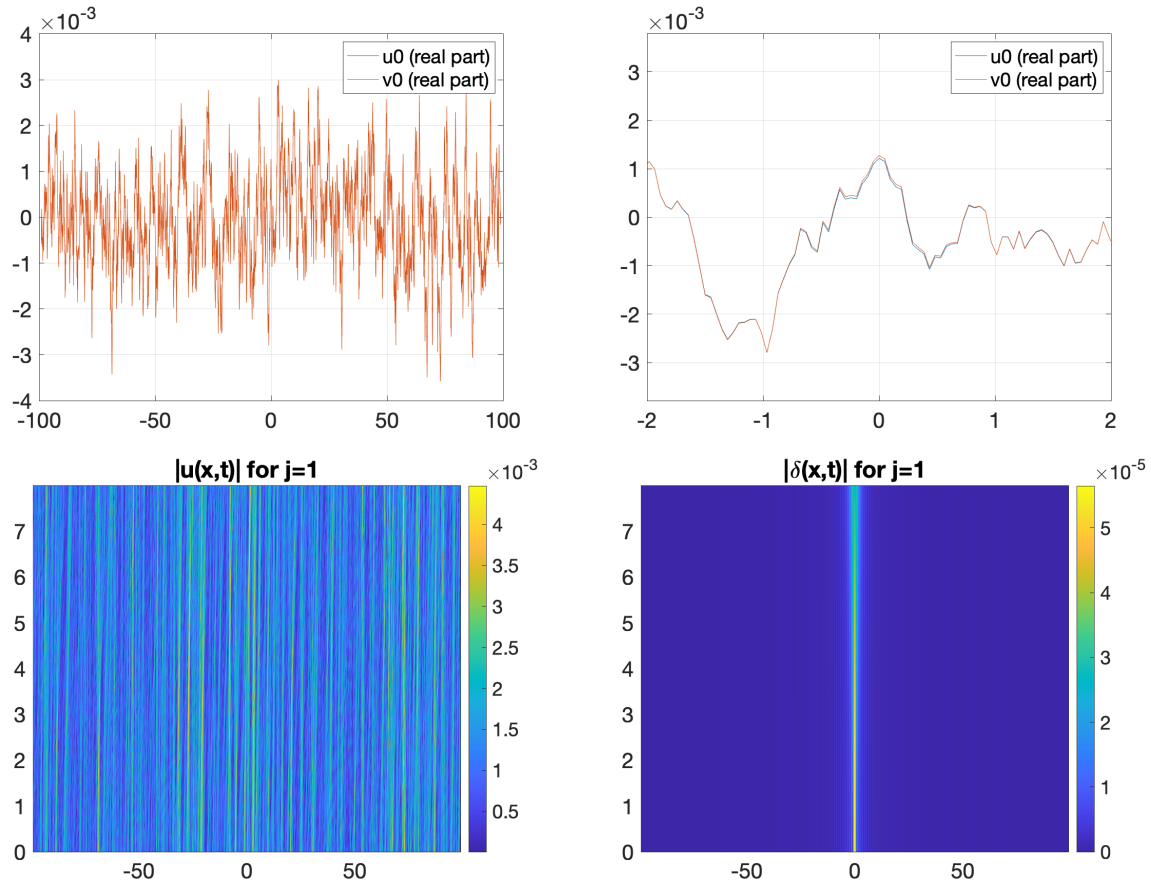


Figure 1: Case $j = 1$. Top left: real parts of initial conditions (global view). Top right: real parts of initial conditions (zoomed around the effective support of the inhomogeneity). Bottom left: modulus of the background solution (see colorbar for values). Bottom right: modulus of the inhomogeneity.

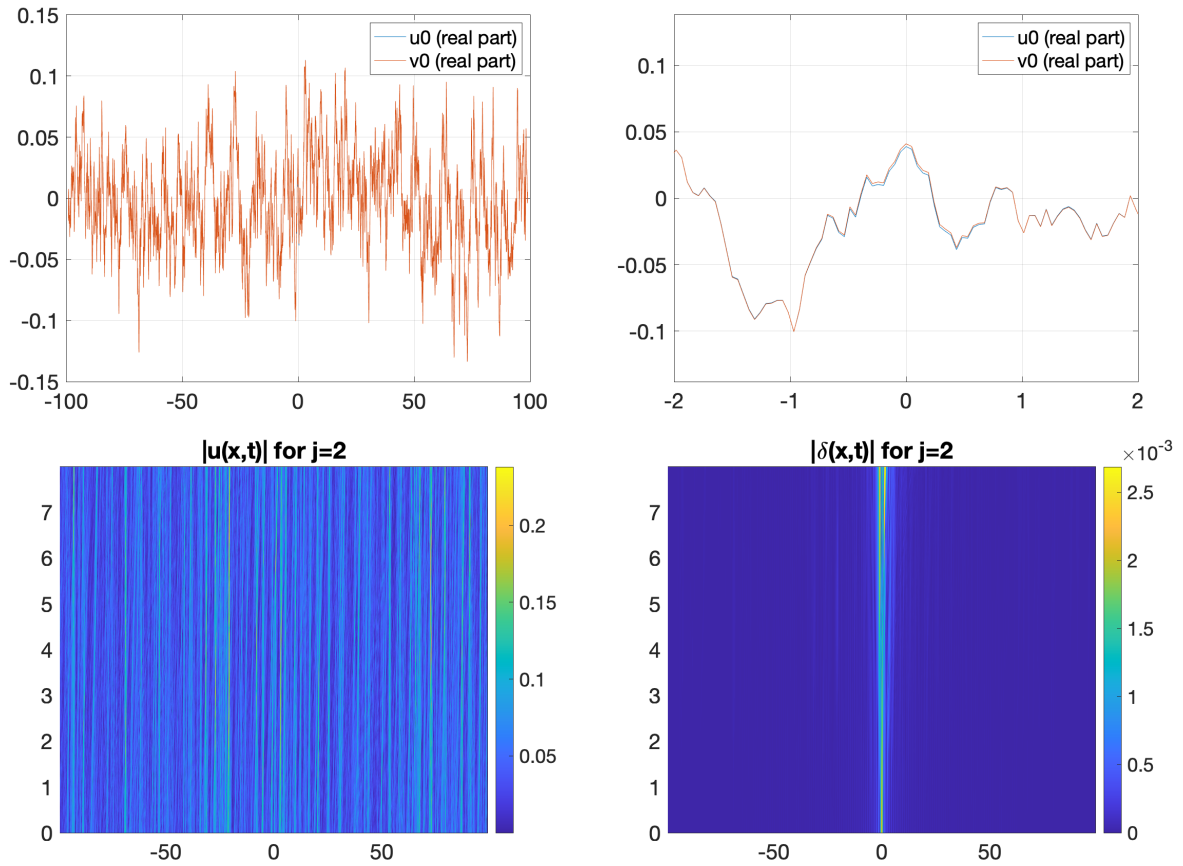


Figure 2: Case $j = 2$. Top left: real parts of initial conditions (global view). Top right: real parts of initial conditions (zoomed around the effective support of the inhomogeneity). Bottom left: modulus of the background solution (see colorbar for values). Bottom right: modulus of the inhomogeneity.

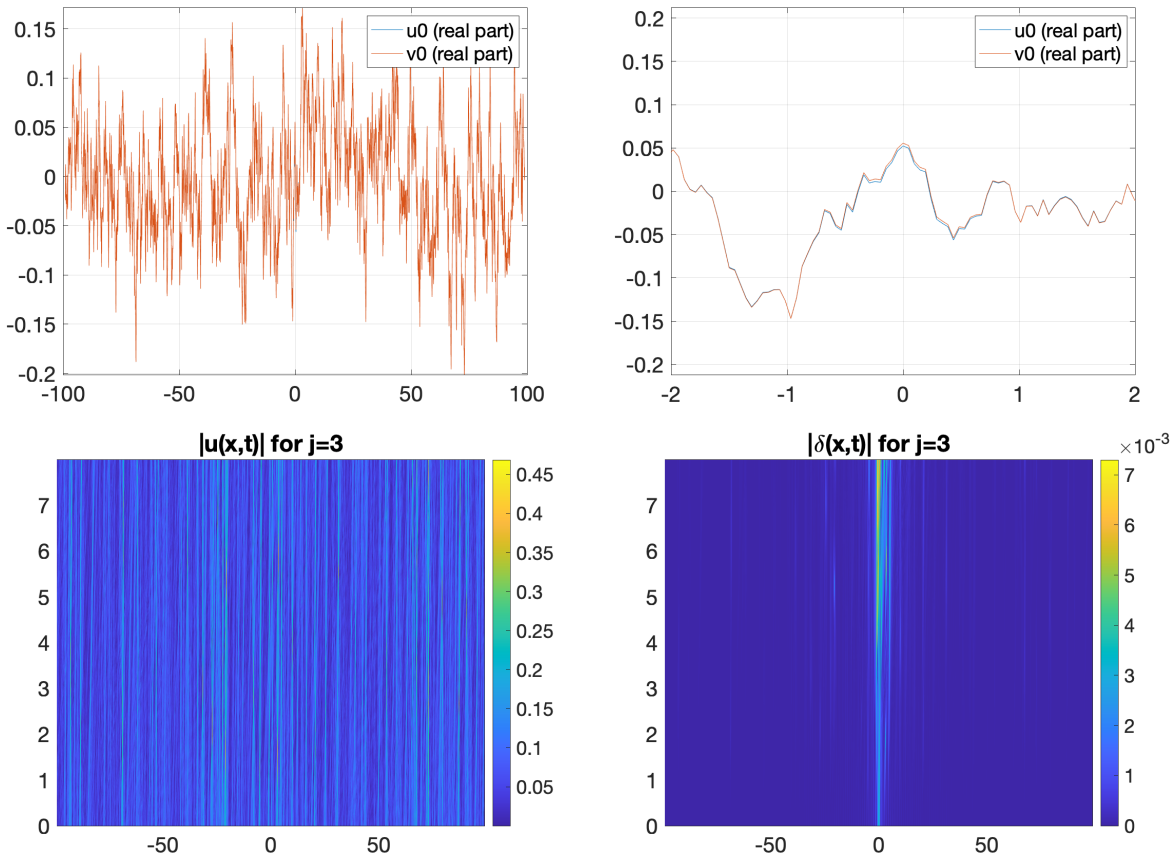


Figure 3: Case $j = 3$. Top left: real parts of initial conditions (global view). Top right: real parts of initial conditions (zoomed around the effective support of the inhomogeneity). Bottom left: modulus of the background solution (see colorbar for values). Bottom right: modulus of the inhomogeneity.

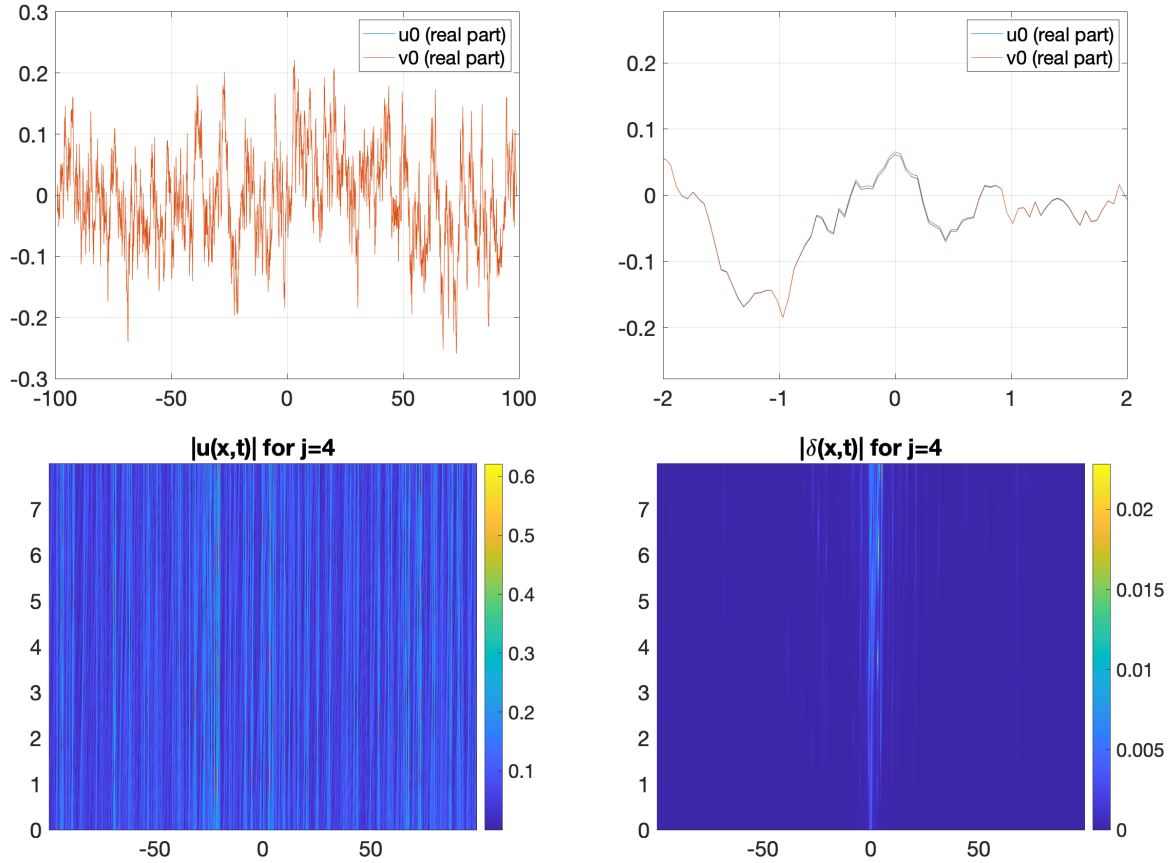


Figure 4: Case $j = 4$. Top left: real parts of initial conditions (global view). Top right: real parts of initial conditions (zoomed around the effective support of the inhomogeneity). Bottom left: modulus of the background solution (see colorbar for values). Bottom right: modulus of the inhomogeneity.

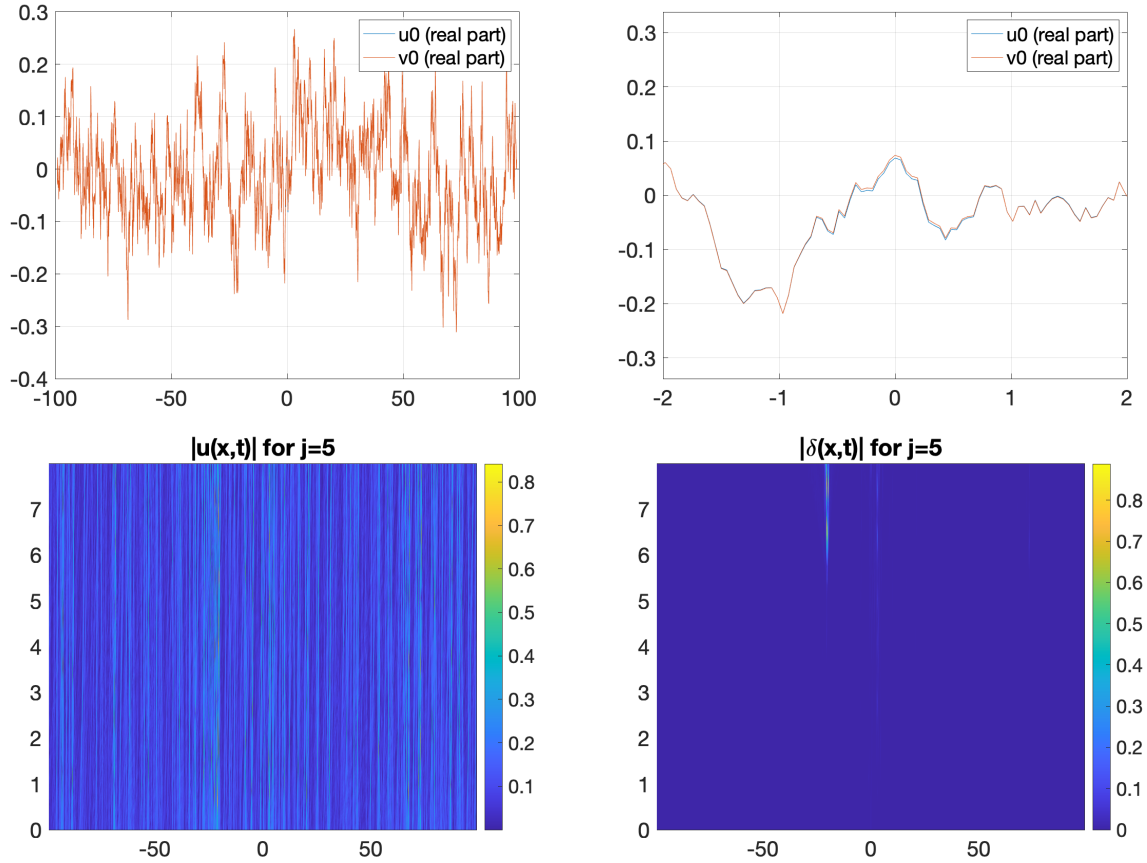


Figure 5: Case $j = 5$. Top left: real parts of initial conditions (global view). Top right: real parts of initial conditions (zoomed around the effective support of the inhomogeneity). Bottom left: modulus of the background solution (see colorbar for values). Bottom right: modulus of the inhomogeneity.

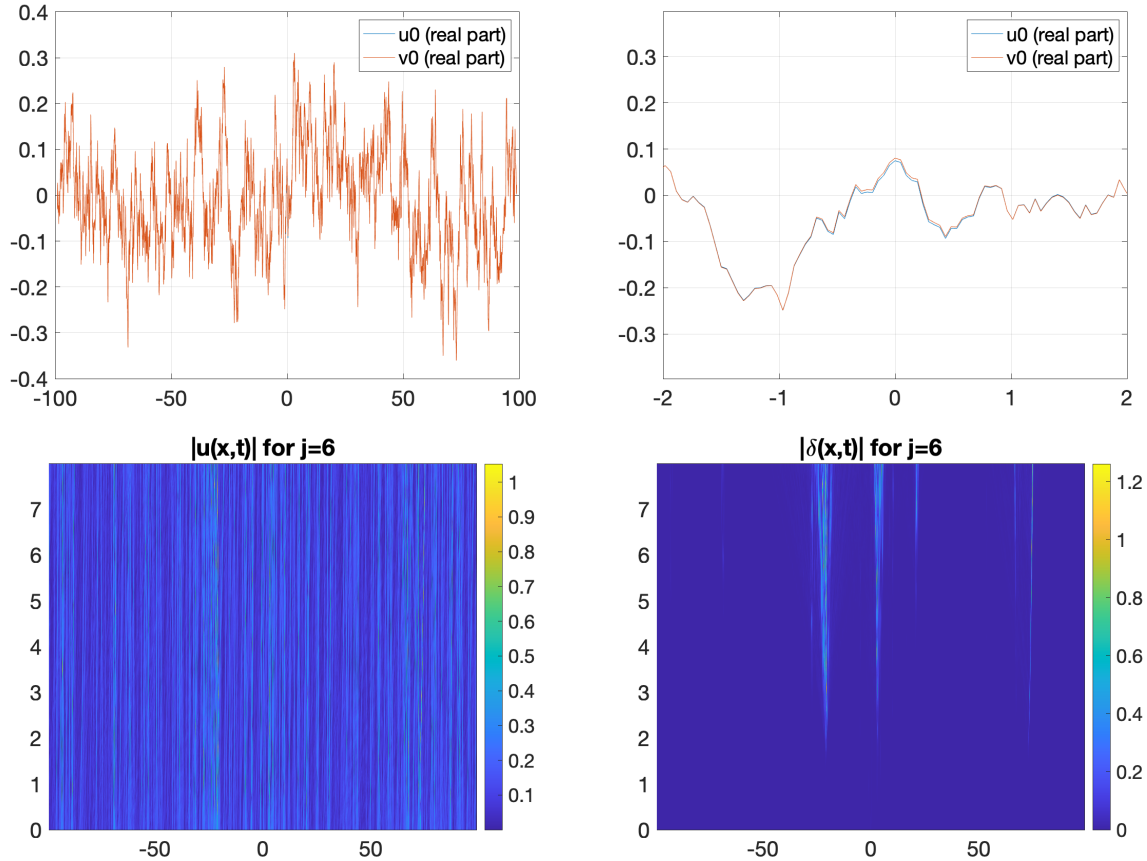


Figure 6: Case $j = 6$. Top left: real parts of initial conditions (global view). Top right: real parts of initial conditions (zoomed around the effective support of the inhomogeneity). Bottom left: modulus of the background solution (see colorbar for values). Bottom right: modulus of the inhomogeneity.

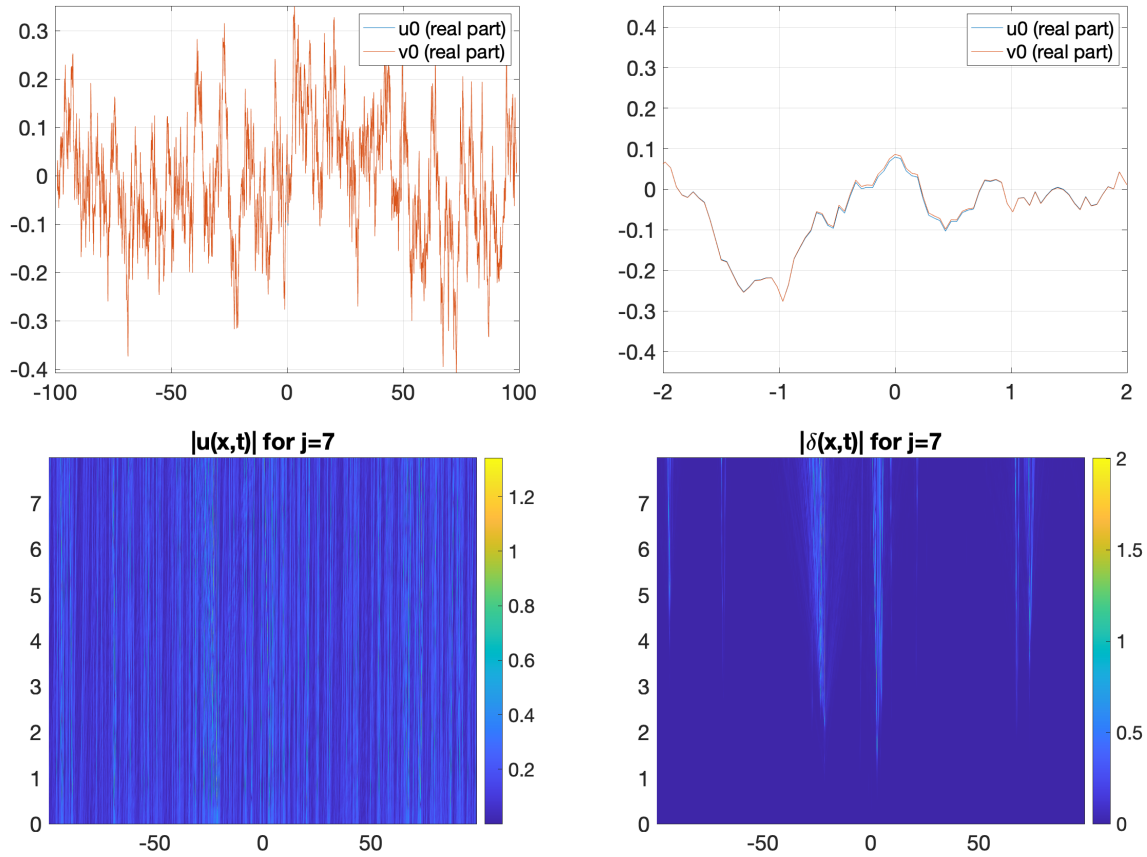


Figure 7: Case $j = 7$. Top left: real parts of initial conditions (global view). Top right: real parts of initial conditions (zoomed around the effective support of the inhomogeneity). Bottom left: modulus of the background solution (see colorbar for values). Bottom right: modulus of the inhomogeneity.